www.nature.com/aps

Acta Pharmacologica Sinica

ARTICLE

DCZ5248, a novel dual inhibitor of Hsp90 and autophagy, exerts antitumor activity against colon cancer

Xiang-ling Chen[1,2], Peng Liu[1], Wei-liang Zhu[1,2] and Li-guang Lou[1,2]

Hsp90 is a potential therapeutic target for tumor, as it maintains the stability of a variety of proteins related to tumor development and progression. Autophagy is a self-degradation process to maintain cellular homeostasis and autophagy inhibitors can suppress tumor growth. In this study, we identified DCZ5248, a triazine derivative, was a dual inhibitor of both Hsp90 and late-autophagy with potent antitumor activity against colon cancer cells in vitro and in vivo. We showed that DCZ5248 (0.1–10 μM) induced dose-dependent degradation of Hsp90 client proteins (AKT, CDK4, CDK6 and RAF-1) in HCT 116 colon cancer cells through a proteasome-dependent pathway. Meanwhile, DCZ5248 (0.3 μM) induced cytoplasmic vacuole formation, LC3 II conversion, p62 protein upregulation, and inhibited autophagy at the late stage in the colon cancer cell lines tested. We further revealed that the inhibition of autophagy was achieved by impairing lysosomal functions through induction of lysosomal acidification and attenuation of lysosomal cathepsin activity. The modulation of autophagy by DCZ5248 was independent of Hsp90 inhibition as the autophagy inhibition was not blocked by Hsp90 knockdown. Importantly, inhibition of both Hsp90 function and autophagy by DCZ5248 induced G_1-phase cell cycle arrest, apoptosis, and exerted potent antitumor activity against colon cancer cells both in vitro and in vivo. These findings demonstrate that DCZ5248 is a novel dual inhibitor of Hsp90 and autophagy with potential for colon cancer therapy.

Keywords: DCZ5248; Hsp90; autophagy; lysosomal function; antitumor activity; colon cancer

Acta Pharmacologica Sinica (2021) 42:132–141; https://doi.org/10.1038/s41401-020-0398-2

INTRODUCTION

Heat shock protein 90 (Hsp90), a kind of molecular chaperone, is widely expressed and highly conserved in cells. Hsp90 is expressed at 2–10 times higher levels in tumor cells than normal cells. It has been reported that the elevated expression of Hsp90 and its client proteins, such as epidermal growth factor receptor (EGFR), AKT, Raf-1, epidermal growth factor receptor 2 (HER2), and cyclin-dependent kinase 4/6 (CDK4/6), are closely related to tumor development and progression [1]. Inhibition of Hsp90 function causes the degradation of client proteins associated with tumors [2]. Therefore, Hsp90 is a promising target for antitumor therapy. Currently, Hsp90 inhibitors in clinical trials mainly bind to the ATP pocket of the N-terminal domain and have high toxicity and low selectivity [3]. Thus, it is urgent to find Hsp90 inhibitors with novel mechanisms of action.

There are three main forms of autophagy: macroautophagy, microautophagy, and chaperone-mediated autophagy [4]. Macroautophagy (hereafter referred to as autophagy) is a form of intracellular lysosomal degradation that produces energy and recycles proteins and organelles. Autophagy consists of a series of events, starting with the inclusion of unwanted cytoplasm into an elongating phagophore to form a double-membrane autophagosome, followed by fusion with lysosomes to generate autolysosomes in which protein digestion occurs [5–7]. Fusion of autophagosomes with lysosomes and protein digestion in autolysosomes are late stages of autophagy. Autophagy can favor tumor cell survival under stress, such as hypoxia, nutrient limitation and certain forms of therapy [4, 8]. Therefore, inhibition of autophagy is a promising strategy for tumor therapy. Currently, the autophagy inhibitor chloroquine (CQ) and its derivative hydroxychloroquine (HCQ) have entered clinical trials for cancer therapy and have displayed signs of efficacy [9].

DCZ5248, a triazine derivative, is a novel Hsp90 inhibitor that directly binds to the Hsp90 protein and does not induce a heat shock response [10]. In the present study, we found that DCZ5248 induced the degradation of client proteins through a proteasome-dependent pathway. Meanwhile, DCZ5248 inhibited autophagy at late stages independent of Hsp90. Importantly, DCZ5248 exerted potent antitumor activity both in vitro and in vivo. These findings demonstrate that DCZ5248 is a novel dual inhibitor of Hsp90 and autophagy and will aid in understanding the regulation of Hsp90 and autophagy and the rational design of triazine for antitumor drugs.

MATERIALS AND METHODS

Reagents and antibodies

DCZ5248 was synthesized by the Shanghai Institute of Materia Medica, Chinese Academy of Sciences (Shanghai, China). Geldanamycin (GM) was purchased from Sangon Biotech (Shanghai, China). Bafilomycin A1 (Baf A1), palbociclib, trametinib and dabrafenib were purchased from Selleckchem (Shanghai, China).

[1]Shanghai Institute of Materia Medica, Chinese Academy of Sciences, Shanghai 201203, China and [2]University of Chinese Academy of Sciences, Beijing 100049, China
Correspondence: Li-guang Lou (lglou@mail.shcnc.ac.cn)

Received: 10 December 2019 Accepted: 15 March 2020
Published online: 13 May 2020

Abemaciclib was from Pharmacodia (Beijing, China). LysoTracker Deep Red was purchased from Thermo Fisher Scientific (Waltham, MA, USA). Propidium iodide (PI), sulforhodamine B and chloroquine were purchased from Sigma-Aldrich (St. Louis, MO, USA). An Annexin V-FITC/PI apoptosis detection kit was purchased from Melonepharma (Dalian, China).

Appropriate antibodies specific for caspase-3, cleaved caspase-3, caspase-9, Rb, p-Rb, AKT, CDK4, CDK6, ULK1, Beclin 1, Atg5, Atg7, Atg12 and LC3 I/II were purchased from Cell Signaling Technology (Beverly, MA, USA). Antibodies against cathepsin B, ERK1/2, RAF-1 and p21 were purchased from Santa Cruz Biotechnology (Santa Cruz, CA, USA). Antibodies against Hsp72 were obtained from Enzo Life Sciences (Farmingdale, NY, USA). Antibodies against cathepsin D were purchased from Wanglebio (Shenyang, China). Antibodies against p62 were purchased from ABclonal Biotechnology (Boston, USA). The antibodies against Hsp90 were from Abcam (Cambridge, UK).

Cell culture

The colon cancer cell lines LS 174T, DIFI, SW480, HCT-15, SW48, LoVo, HCT 116, HT-29 and SW620 were purchased from American Type Culture Collection (Manassas, VA, USA) and cultured according to the instructions provided by the supplier.

Cell proliferation assay

Tumor cells were seeded onto 96-well plates, cultured overnight, and then treated with increasing concentrations of compounds (in triplicate) for 120 h. Antiproliferative activity was assessed using sulforhodamine B (SRB; Sigma) assays, as described previously [11].

Western blot assay

After drug treatment, cells were collected and lysed in sodium dodecyl sulfate (SDS) sample buffer (100 mM Tris-HCl, pH 6.8, 2% SDS, 20% glycerol, 1 mM dithiothreitol). Equal amounts of proteins were resolved by sodium dodecyl sulfate polyacrylamide gel electrophoresis (SDS-PAGE), transferred to polyvinylidene difluoride (PVDF) membranes, probed with primary antibodies, and then incubated with the appropriate secondary antibodies (Millipore). Immunoreactive bands were visualized using enhanced chemiluminescence reagents (Millipore).

siRNA transfection

For siRNA studies, cells were transfected with siRNAs against Hsp90 (Hsp90α/β#1, Hsp90α/β#2) or negative control siRNA (GenePharma, Shanghai, China) using the Lipofectamine 2000 transfection reagent (Thermo-Fisher Scientific). The sequences of these siRNAs are as follows:

Hsp90A sense: 5′-CGUGAGAUGUUGCAACAAAtt-3′,
antisense: 5′-UUUGUUGCAACAUCUCACGtt-3′,
Hsp90B sense: 5′-CCUGUUCAGUACUCUACAAtt-3′,
antisense: 5′-UUGUAGAGUACUGAACAGGtt-3′,
Hsp90C sense: 5′-GAAGACAAGGAGAAUUACAtt-3′,
antisense: 5′-UGUAAUUCUCCUUGUCUUCtt-3′,
Hsp90D sense: 5′-GCAAGGCAAAGUUUGAGAAtt-3′,
Antisense: 5′-UUCUCAAACUUUGCCUUGCtt-3′.

Strands A and B are specific to Hsp90α. Strands C and D are specific to Hsp90β.

Neutral red and acridine orange staining

Cells were plated onto 6-well plates and cultured overnight. After treatment with DCZ5248 for 12 h, cells were stained with 1 μg/mL acridine orange (AO) or 28 μg/mL neutral red (NR) for 30 min at 37 °C. For NR staining, images were captured using an Olympus fluorescence microscope, and for AO staining, acidic vacuoles were quantified by an Accrui-C6 plus flow cytometer (BD Biosciences, San Jose, CA, USA).

Establishment of a cell line stably expressing the mCherry-GFP-LC3 protein

HT-29 cells were transfected with plasmids pmCherry-C1-GFP-LC3 using Lipo 2000 reagent. Cells were selected with 1 mg/mL G418, and monoclonal cells expressing mCherry-GFP-LC3 protein were isolated by serial dilution.

Fluorescence microscopy

HT-29 cells stably expressing mCherry-GFP-LC3 were treated with DCZ5248 for 12 h and then fixed with 4% paraformaldehyde, and images were taken using an Olympus FV1000 confocal microscope (Tokyo, Japan). For acidification experiments, cells were treated with DCZ5248 for 12 h, stained with LysoTracker Deep Red (50 nM), fixed with 4% paraformaldehyde, and observed under an Olympus FV1000 confocal microscope.

Flow cytometry analysis

Cells were harvested and fixed in ice-cold 70% ethanol at −20 °C overnight. Fixed cells were then treated with 50 μg/mL propidium iodide and RNase A at 37 °C for 30 min. The cell cycle distribution was measured using a FACScan flow cytometer (BD Biosciences, San Jose, CA, USA) and analyzed with ModFit LT Mac V3.0 software. Apoptosis was measured using an Annexin V-FITC Apoptosis Detection Kit according to the manufacturer's instructions. Fluorescence was acquired with an Accuri C6 Plus instrument (BD Biosciences).

In vivo study

Female Balb/cA-nude mice (5–6 weeks old) were purchased from the Shanghai Laboratory Animal Center (Shanghai, China). Human tumor xenografts were prepared by subcutaneously implanting HT-29 cells in the right flank of the animal. When tumor volumes reached ~100 mm^3, mice were randomly assigned to control ($n = 10$) or treatment ($n = 6$) groups and intraperitoneally injected with DCZ5248 daily for 17 days at doses of 35 or 70 mg/kg. Tumor volume was calculated as $(\text{length} \times \text{width}^2)/2$. The therapeutic effect of a given compound was expressed in terms of tumor growth inhibition (TGI), calculated as $TGI = (Vt' - Vt)/(Vc' - Vc) \times 100\%$, where Vt′ and Vt are the tumor volumes in treatment groups on each day of measurement and on the day of initial treatment, respectively, and Vc′ and Vc are the tumor volumes in the vehicle control group on each day of measurement and on the day of initial treatment, respectively.

Animal experiments were conducted in accordance with the guidelines of the Institutional Animal Care and Use Committee at the Shanghai Institute of Materia Medica, Chinese Academy of Sciences.

Data analysis

Data are presented as the means ± SD and were plotted using GraphPad Prism Version 5. Student's *t*-test was used to determine significance, where indicated. Differences were considered significant at $P < 0.05$.

RESULTS

DCZ5248 degrades client proteins through a proteasome-dependent pathway

A previous study reported that DCZ5248 is a novel Hsp90 inhibitor (Fig. 1a) [10]. In this study, we further investigated the effect of DCZ5248 on the expression of client proteins, including AKT, CDK4, CDK6 and RAF-1. DCZ5248 downregulated the expression of these proteins in a concentration- and time-dependent manner in the colon cancer HCT 116 cell line (Fig. 1b, c). It has been reported that the degradation of client proteins caused by Hsp90 inhibitors is mediated by proteasomes [12, 13]. Our study shows that the downregulation of client proteins caused by DCZ5248 was reversed by MG132, a well-characterized proteasome inhibitor

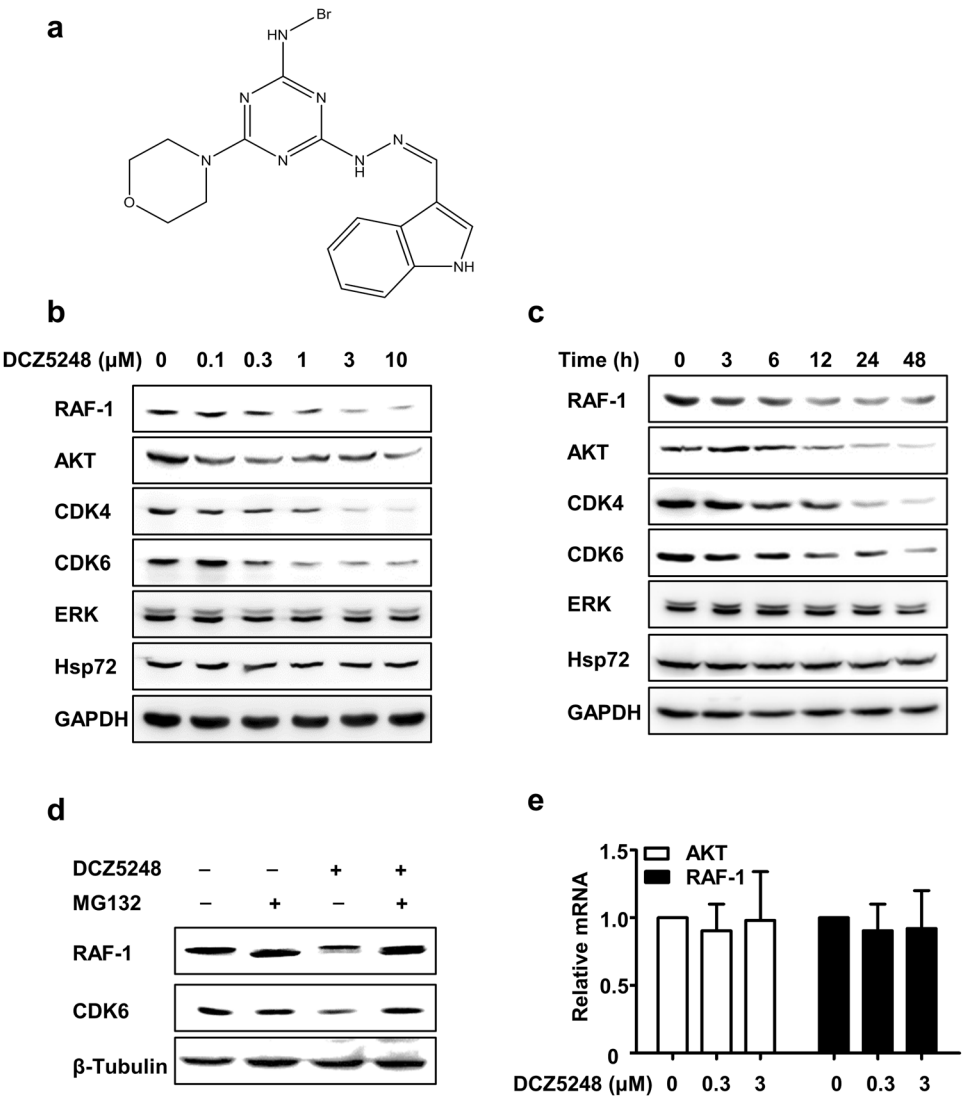

Fig. 1 DCZ5248 induces client protein degradation via a proteasome-dependent pathway. **a** Chemical structure of DCZ5248. **b** HCT 116 cells were treated with DCZ5248 for 12 h. Whole-cell lysates were analyzed by Western blotting using the indicated antibodies. **c** HCT 116 cells were treated with 1 μM DCZ5248 for different periods of time. Whole-cell lysates were analyzed by Western blotting using the indicated antibodies. **d** HCT 116 cells were pretreated with 1 μM MG132 for 2 h and then incubated in the presence or absence of 1 μM DCZ5248 for an additional 12 h. Whole-cell lysates were analyzed by Western blotting using the indicated antibodies. **e** HCT 116 cells were treated with DCZ5248 for 12 h. Total RNA was extracted, and AKT and RAF-1 mRNA levels were determined by quantitative real-time PCR; GAPDH was used as an internal control. Data are presented as the means ± SD (error bars; $n = 3$)

(Fig. 1d). Furthermore, the transcription of client proteins such as AKT and RAF-1 was not significantly inhibited by treatment with DCZ5248 (Fig. 1e). These results showed that DCZ5248, as an Hsp90 inhibitor, indeed induced the degradation of Hsp90 client proteins via a proteasome-dependent pathway.

DCZ5248 inhibits autophagy at the late stage

DCZ5248 induced cytoplasmic vacuole formation in all tested colon cancer cell lines (SW48, SW480, SW620, LS 174T, LoVo, HCT 116, HT-29 and HCT-15) when cells were treated with DCZ5248 for 12 h at a concentration of 0.3 μM (Supplementary Fig. S1a). To further understand the mechanisms of vacuole formation, we tested the effect of DCZ5248 on the specific autophagy biomarker LC3. DCZ5248 significantly increased the LC3 I to LC3 II conversion, suggesting that DCZ5248 may modulate the process of autophagy in colon cancer cells (Supplementary Fig. S1b).

To further investigate the modulation of DCZ5248 on autophagy, we measured the expression of a few autophagy-related factors in HT-29 cells. DCZ5248 increased the level of p62 in a concentration-dependent manner, but had no significant effect on other factors, such as Beclin 1, ULK1, Atg 5, Atg 7 and Atg 12 (Fig. 2a). It has been reported that p62 is degraded at the late stage of autophagic flux, and the accumulation of p62 can be regarded as a marker for the inhibition of autophagic flux [14, 15]. Furthermore, we compared the effect of the well-known autophagy inducer rapamycin and the autophagy inhibitor CQ on the expression of LC3 II and p62. All tested drugs increased LC3 II conversion. However, the autophagy inducer rapamycin decreased the expression of p62, while DCZ5248 increased the expression of p62, which is consistent with the autophagy inhibitor CQ (Fig. 2b). These data collectively suggested that DCZ5248 could inhibit autophagy flux at the late stage.

To clarify the modulation of DCZ5248 on autophagy flux, we established the cell line HT-29 stably expressing mCherry-GFP-LC3. The probe mCherry-GFP-LC3 results in both green and red fluorescence and is used to identify autophagosomes and

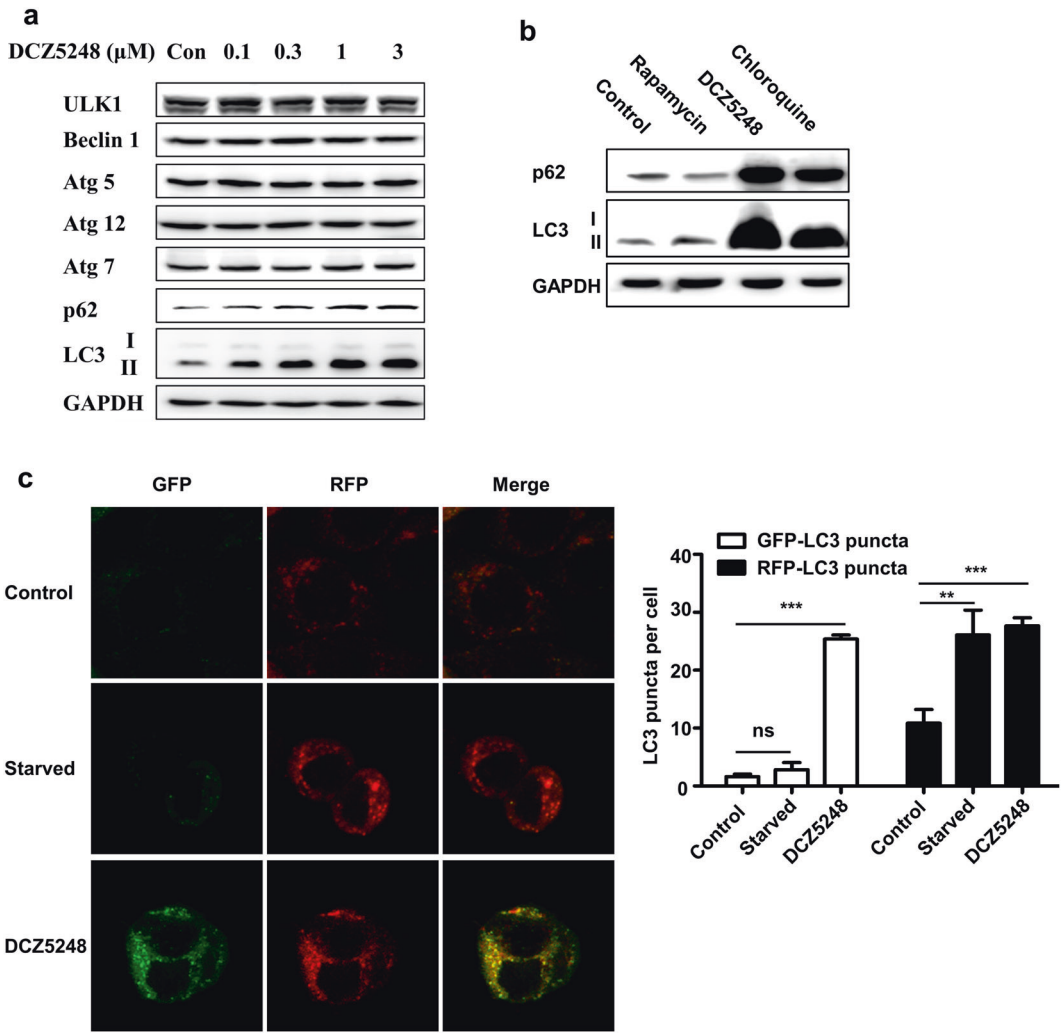

Fig. 2 DCZ5248 inhibits autophagy flux. **a** HT-29 cells were treated with DCZ5248 for 12 h, and whole-cell lysates were analyzed by Western blotting. **b** HT-29 cells were treated with DMSO, 1 μM rapamycin, 0.3 μM DCZ5248 or 50 μM chloroquine, and whole-cell lysates were analyzed by Western blotting. **c** HT-29 cells stably expressing mCherry-GFP-LC3 were treated with DMSO, serum-free culture medium (starved) or 0.3 μM DCZ5248 for 12 h. Paraformaldehyde-fixed cells were visualized by confocal microscopy. Magnification: 1000×. The bar chart shows the number of LC3 puncta per cell. $^{**}P < 0.01$, $^{***}P < 0.001$, compared with control; ns, no significance

autolysosomes because GFP fluorescence is quenched in acidic compartments, whereas mCherry is more stable in low pH environments. Thus, if autolysosome maturation proceeds normally or flux is increased, the red-only puncta will increase. In contrast, if the autophagosome does not fuse with lysosomes or lysosomal function is impaired, the yellow puncta will increase in the merged image. HT-29 cells exhibited an increase in both red and yellow punctate fluorescence upon DCZ5248 treatment, whereas there was only an increase in red punctate fluorescence upon starvation treatment (Fig. 2c). These results demonstrated that DCZ5248 induced the accumulation of autophagosomes and autolysosomes and inhibited autophagy at the late stage.

DCZ5248 inhibits autophagy through impairment of lysosomal functions

The above results suggested that the impaired autophagy flux induced by DCZ5248 might be involved in the functions of the lysosome. Thus, we examined the effects of DCZ5248 on lysosomal functions. AO and NR are two dyes for staining the acidic organelles of cells. The red fluorescence of AO measured by flow cytometry was significantly upregulated in DCZ5248-treated HT-29 and HCT 116 cells in a time-dependent manner (Fig. 3a). Consistent with this, the red staining of NR observed under a fluorescence microscope was increased after DCZ5248 treatment of cells (Fig. 3b). LysoTracker Deep Red is an acidic pH marker for lysosomes. Confocal microscopy of DCZ5248-treated cells showed significant LysoTracker Deep Red signals compared to control cells (Fig. 3c). AO, NR and LysoTracker Deep Red staining indicated that there were increased acidic components after DCZ5248 treatment. When cells were treated with DCZ5248 combined with Baf A1, a lysosomal lumen alkalizer, the acidic cell components and vacuolization were reversed (Fig. 3a, c). Thus, the abnormally low pH of lysosomes was required for vacuolization, and DCZ5248 induced lysosomal acidification.

A key step in the autophagic process is the degradation of cargo in autolysosomes. We wondered whether DCZ5248 treatment affected lysosomal activity. Cathepsin proteases are important lysosomal hydrolases that degrade the sequestered components. We investigated the effects of DCZ5248 on cathepsin processing by immunoblotting using antibodies specific for the pro-form and the mature form of cathepsin B or cathepsin D. DCZ5248 significantly impaired the maturation of cathepsin B and cathepsin D in a concentration-dependent manner (Fig. 3d). Next, we tested whether the effect of DCZ5248 on the maturation of cathepsin B and

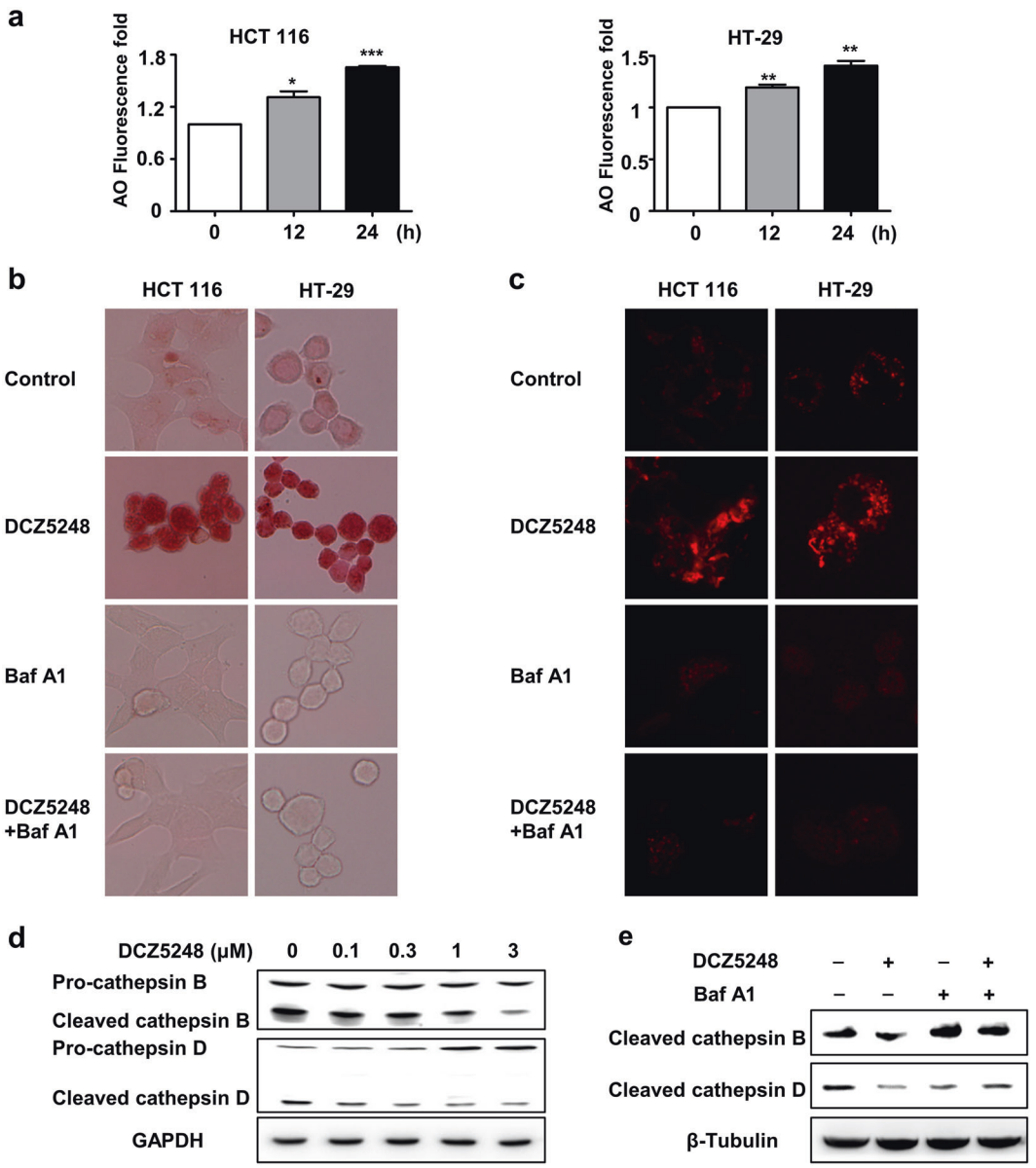

Fig. 3 DCZ5248 impairs lysosomal functions. **a** HCT 116 or HT-29 cells were treated with DCZ5248 for different periods of time and then stained with the acidification indicator acridine orange (AO). *$P < 0.05$, **$P < 0.01$, ***$P < 0.001$, vs. control. **b** HCT 116 or HT-29 cells were treated with 0.3 μM DCZ5248, 10 nM Baf A1, or in combination for 12 h and then stained with neutral red for 30 min. Magnification: 400×. **c** HCT 116 or HT-29 cells were treated with 0.3 μM DCZ5248, 10 nM Baf A1, or in combination for 12 h and then stained with LysoTracker Red for 1 h. Paraformaldehyde-fixed cells were visualized by confocal microscopy. Magnification: 1000×. **d** HT-29 cells were treated with DCZ5248 for 12 h. Whole-cell lysates were analyzed by Western blotting using the indicated antibodies. **e** HT-29 cells were treated with 3 μM DCZ5248, 10 nM Baf A1 or in combination for 12 h, and whole-cell lysates were analyzed by Western blotting

cathepsin D could be reversed by Baf A1. We observed that the effect of DCZ5248 on the maturation of cathepsin proteases was reversed by Baf A1 (Fig. 3e). Taken together, these data suggested that DCZ5248 induced lysosomal acidification and attenuated lysosomal cathepsin activity to impair lysosomal function, and then resulted in the inhibition of autophagy.

Inhibition of autophagy by DCZ5248 is independent of Hsp90

DCZ5248 induced vacuole formation, whereas the traditional Hsp90 inhibitor GM did not (Fig. 4a). In addition, DCZ5248 induced the upregulation of p62, whereas GM decreased the protein level of p62 (Fig. 4b). These data suggest that DCZ5248 inhibition of autophagy may not be through Hsp90 inhibition.

To determine the role of Hsp90 in the DCZ5248 inhibition of autophagy, we next knocked down Hsp90 using Hsp90-target siRNA. Transfection of HT-29 cells with two different Hsp90-target siRNAs, Hsp90α/β#1 and Hsp90α/β#2, decreased Hsp90 expression (Fig. 4c, left panel). However, knocking down Hsp90 with siRNA did not cause vacuolization (Fig. 4c, right panel). DCZ5248 still effectively induced vacuolization, p62 upregulation and LC3 II conversion when HT-29 cells were transfected with Hsp90-target siRNAs and Hsp90 was knocked down (Fig. 4d), suggesting that inhibition of autophagy by DCZ5248 was independent of Hsp90.

To confirm this, we used the cell line HT-29 expressing mCherry-GFP-LC3 to further investigate the effect of DCZ5248 on autophagy when Hsp90 was knocked down. DCZ5248 effectively inhibited autophagy flux in HT-29 cells transfected with Hsp90-target siRNAs or negative siRNA, as cells exhibited an increase in both red and yellow punctate fluorescence upon DCZ5248

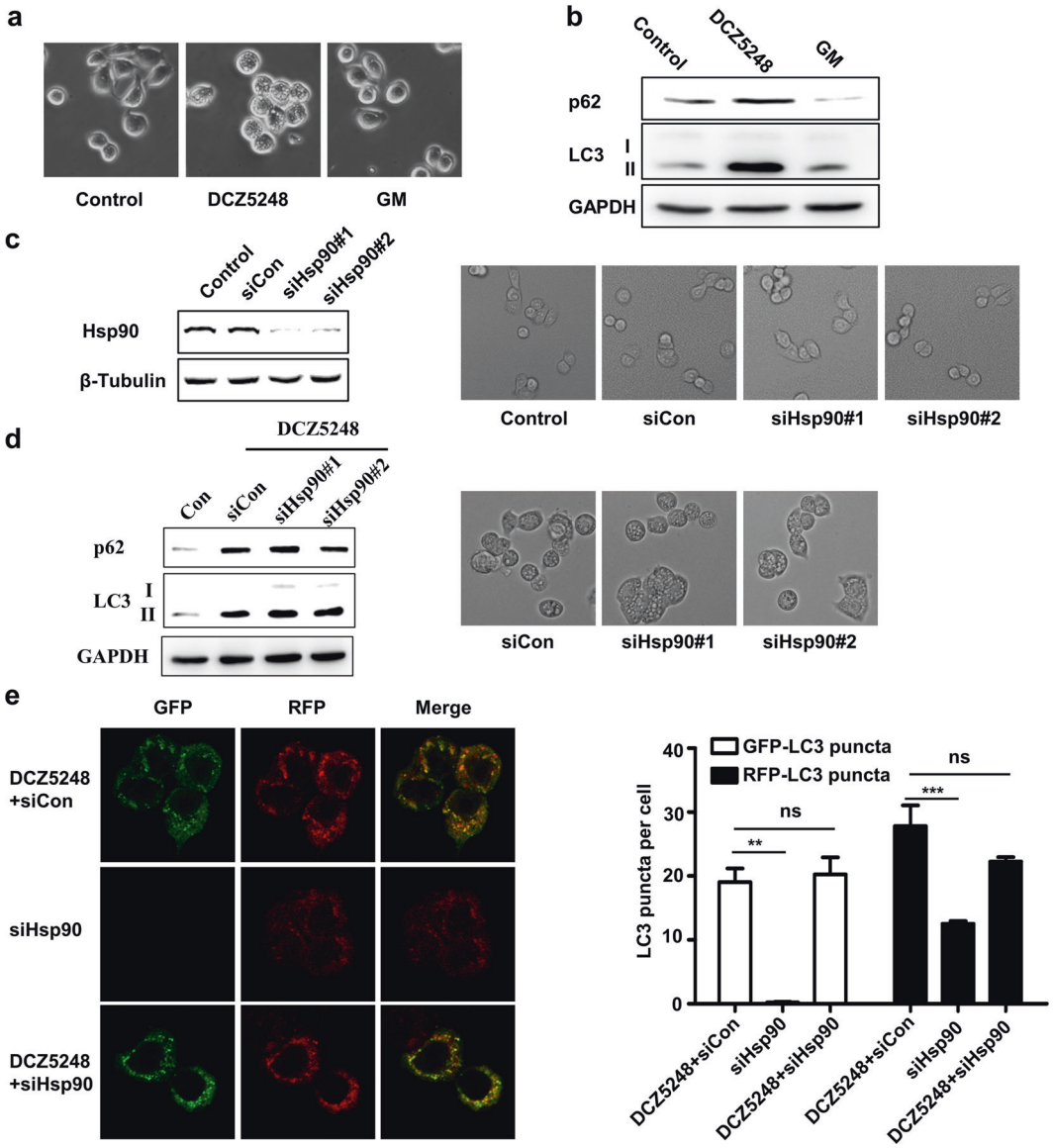

Fig. 4 The inhibition of autophagy by DCZ5248 is independent of Hsp90. **a** HT-29 cells were treated with 0.3 μM DCZ5248 or 0.1 μM geldanamycin (GM) for 12 h. Phase-contrast images were taken at a magnification of 200×. **b** HT-29 cells were treated with 0.3 μM DCZ5248 or 0.1 μM GM for 12 h, and whole-cell lysates were analyzed by Western blotting. **c** After transfecting HT-29 cells with Hsp90-target siRNA (siHsp90#1, siHsp90#2) or control siRNA (siCon), whole-cell lysates were analyzed by Western blotting using Hsp90 antibody. Phase-contrast images were taken at a magnification of 200×. **d** HT-29 cells transfected with Hsp90-target siRNA or control Hsp90 siRNA were treated with 0.3 μM DCZ5248. Whole-cell lysates were analyzed by Western blotting using the indicated antibodies. Phase-contrast images were taken at a magnification of 200×. **e** HT-29 cells stably expressing mCherry-GFP-LC3 were transfected with Hsp90-target siRNA or control Hsp90 siRNA and treated with 0.3 μM DCZ5248 for 12 h. Fixed cells were visualized by confocal microscopy. Magnification: 1000×. The bar chart shows the number of LC3 puncta per cell. $^{**}P < 0.01$, $^{***}P < 0.001$; ns, no significance

treatment (Fig. 4e). These results indicated that autophagy inhibition caused by DCZ5248 was not through Hsp90 inhibition.

DCZ5248 inhibits cell proliferation and induces cell cycle arrest and apoptosis

The antiproliferative activity of DCZ5248 in vitro was examined in a panel of colon cancer cell lines. DCZ5248 significantly inhibited cell proliferation, with IC_{50}s ranging from 107.7 to 619.5 nM (Table 1). We next examined the effects of DCZ5248 on the cell-cycle profile. In HCT 116 and HT-29 cells exposed to DCZ5248, cells were arrested in G_1 phase; upon 3 μM DCZ5248 treatment for 48 h, the G_1-phase proportion of cells in these two lines increased from 74.5% to 91.7% and from 77.2% to 91.0%, respectively (Fig. 5a, b). Consistent with this, G_1-phase-related proteins, such as Rb and p-Rb, were downregulated, and p21 was upregulated (Fig. 5b). We then proceeded to test the effect of DCZ5248 on apoptosis in colon cancer cells. Treatment with DCZ5248 for 72 h caused concentration-dependent apoptosis in both HCT 116 and HT-29 cell lines (Fig. 6a, b). The induction of apoptosis by DCZ5248 was further evidenced by the cleavage of caspase-3 and caspase-9 (Fig. 6c). Taken together, these findings indicated that DCZ5248 exerted potent antitumor activity against colon cancer cells in vitro.

DCZ5248 exhibits in vivo antitumor activity in colon cancer xenografts

Given the encouraging antitumor activity against colon cancer in vitro, we next tested the antitumor efficacy of DCZ5248 in vivo. DCZ5248 inhibited the growth of HT-29 xenografts in mice in a

dose-dependent manner at doses of 35 mg/kg and 70 mg/kg. DCZ5248 at a dose of 70 mg/kg inhibited tumor growth by 41% ($P < 0.01$) on the final treatment day (Fig. 7a). These mice tolerated the treatments well, as evidenced by the absence of significant body weight loss during the course of the experiment in all groups (Fig. 7b). The antitumor effects of DCZ5248 were accompanied by the degradation of the Hsp90 client proteins AKT, RAF-1, CDK4 and CDK6 and the accumulation of autophagic marker LC3 II conversion and p62 (Fig. 7c), suggesting that the antitumor activity of DCZ5248 is achieved, at least in part, through inhibiting both Hsp90 and autophagy.

Table 1. Anti-proliferative activity of DCZ5248 against colon cell lines

Cell lines	DCZ5248 (nM, $IC_{50} \pm SD$)
LS 174T	107.7 ± 17.6
DIFI	619.5 ± 36.7
SW480	562.6 ± 8.8
HCT-15	240.7 ± 99.9
SW48	108.8 ± 37.2
LOVO	152.2 ± 88.8
HCT 116	283.9 ± 64.1
HT-29	111.1 ± 4.9
SW620	306.9 ± 101.2

Different cells were plated in 96-well plates and incubated with different concentrations of DCZ5248 for 120 h in triplicate. GraphPad Prism 5 software was used to calculate IC_{50} values. Values represent means ± SD ($n = 3$)

DISCUSSION

Cancer cells adapt to metabolic stress resulting from accelerated cell growth and a lack of nutrients. Hsp90, which is highly expressed in cancer cells, regulates the stability of client proteins, including HER2, AKT, and CDK4, and most client proteins are oncoproteins essential for cancer cell survival and proliferation in the face of metabolic stress [1, 2, 16, 17]. Therefore, targeting Hsp90 is a promising strategy for the treatment of cancer. A previous study reported that DCZ5248 is a novel Hsp90 inhibitor that directly binds to different sites of the Hsp90 from where traditional Hsp90 inhibitors bind to. In this study, we further confirmed that DCZ5248 degraded Hsp90 client proteins through a proteasome-dependent pathway. Hsp90 inhibitors such as SNX-2112, geldnamycin (GM) and BIIB021 have been reported to induce autophagy in different cells [18–20]. However, DCZ5248

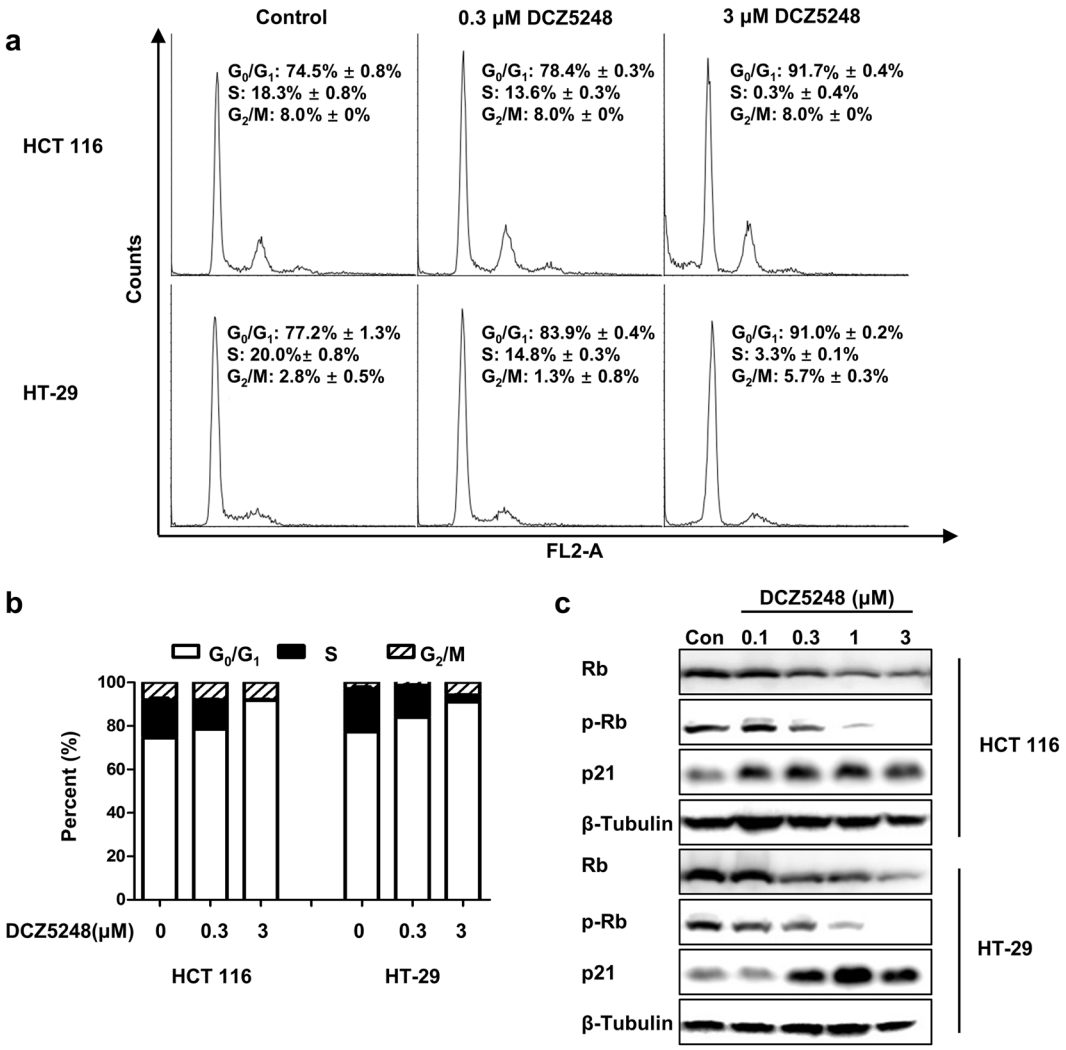

Fig. 5 DCZ5248 induces G_1-phase cell cycle arrest. **a**, **b** Cells were treated with DCZ5248 for 48 h, and the cell cycle distribution was determined by flow cytometry. **c** After treatment of cells with DCZ5248 for 48 h, whole-cell lysates were analyzed by Western blotting

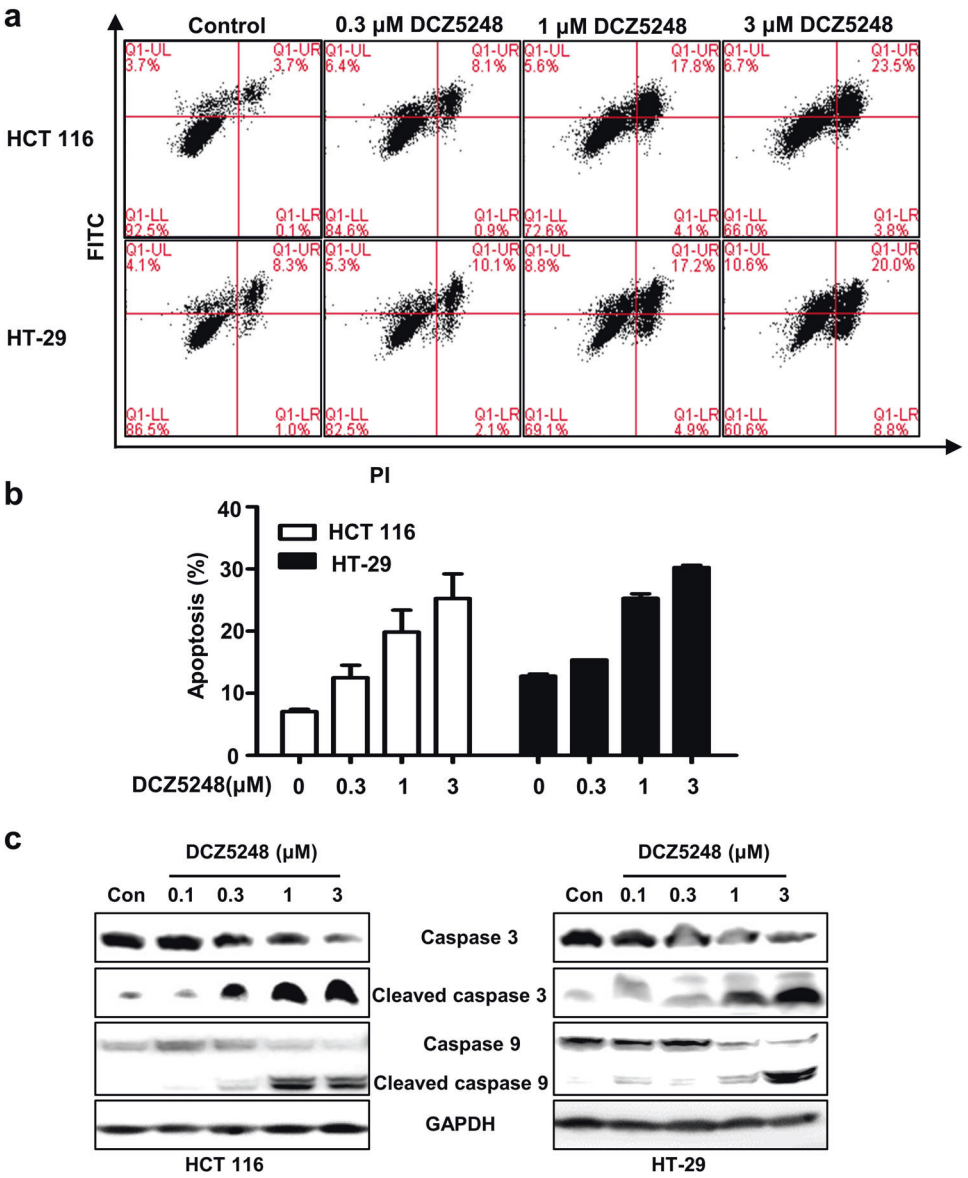

Fig. 6 DCZ5248 induces apoptosis in colon cancer cells. **a**, **b** HCT 116 and HT-29 cells were treated with DCZ5248 at the indicated concentrations for 72 h, stained with annexin V-FITC/PI, and analyzed by flow cytometry. **c** After treatment of cells with DCZ5248 for 72 h, whole-cell lysates were analyzed by Western blotting

was found to inhibit autophagy independent of Hsp90, which may aid in understanding Hsp90 and autophagy.

Autophagy functions under stress, such as hypoxia, nutrient limitation and certain forms of therapy. Cancer cells might upregulate autophagy due to their metabolic dependency on the catabolic process for survival. At the late stage of autophagy, lysosomes maintain a suitable acidic lumen (pH 4.5–5.0) for proteolysis to keep their function active [21]. R428 and SB202190 were previously reported to induce lysosomal acidification, resulting in inhibition of autophagy [7, 22]. Our data demonstrated that DCZ5248 also induced lysosomal acidification. Furthermore, DCZ5248 attenuated lysosomal cathepsin activity, which is important for degrading the sequestered components. Thus, DCZ5248 belonged to the late-stage autophagy inhibitor group due to its impairment of lysosomal function. Late-stage autophagy inhibitors have proven to be useful adjuvants in many antitumor therapies [23, 24]. Considering that both autophagy and Hsp90 function are involved in tumor growth, it is believed that DCZ5248, as a novel dual inhibitor of Hsp90 and autophagy, will have potential for cancer therapy and that inhibition of both Hsp90 and autophagy can serve as a new therapeutic strategy for cancer.

Activation of autophagy as a prosurvival mechanism may reduce the efficacy of various therapeutic regimens [25] and even serve as a stress adaptation causing tumor resistance to chemotherapy and radiotherapy. A variety of drugs have been reported to cause cancer cell death in cancers by inhibiting the autophagy pathway [26–32]. Additionally, radiotherapy, chemotherapy and other kinase inhibitors have been reported to have synergistic antitumor activity with Hsp90 inhibitors [33–35]. For example, HCQ has been evaluated in several phase I and II clinical trials in combination with chemotherapy drugs in a variety of tumor types [36–39], and the Hsp90 inhibitors AT13387, 17-aminogeldanamycin, ganetespib, and AUY922 sensitize tumor cells to B-RAF inhibitors, MEK inhibitors, EGFR inhibitors, HER2 inhibitors, etc. [3, 40–43]. Therefore, the combination of an autophagy inhibitor with an Hsp90 inhibitor may synergistically resensitize tumor cells to chemotherapy or other cancer therapies. DCZ5248, which inhibited both Hsp90 function and autophagy,

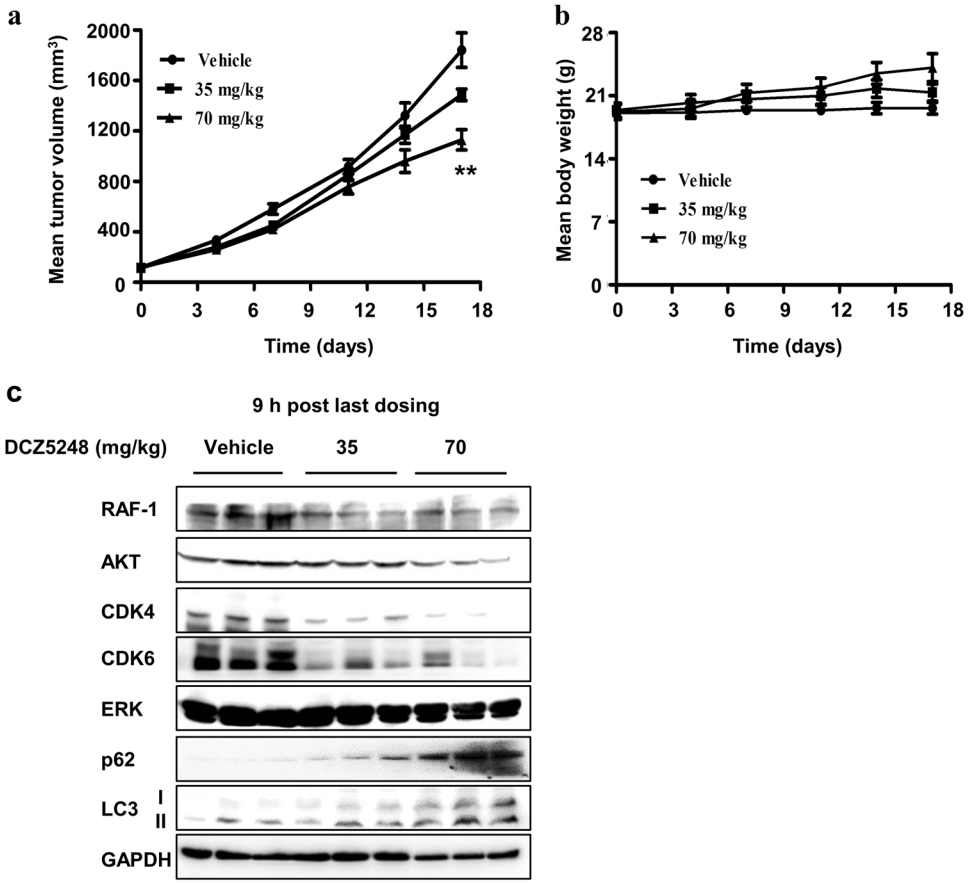

Fig. 7 DCZ5248 exerts antitumor activity in vivo. **a**, **b** HT-29 tumor-bearing mice were intraperitoneally administered DCZ5248 daily for 17 days. Tumor volumes and body weight were measured twice a week. $^{**}P < 0.01$ vs vehicle. **c** Mice were sacrificed 9 h after the last dosing, and tumors were removed and analyzed by Western blotting

not only exerted potent antitumor activity against a series of colon cancer cell lines but also efficiently sensitized cancer cells to multiple drugs, such as the CDK4/6 inhibitor abemaciclib or palbociclib, the MEK inhibitor trametinib and the B-RAF (V600E) inhibitor dabrafenib (Supplementary Fig. S2). Therefore, inhibition of Hsp90 and autophagy may be an effective approach for the treatment of cancers.

Although the 5-year survival rate of patients with colon cancer is on the rise, the total death toll is still very high. Both Hsp90 and autophagy favor tumor cell survival under stress, and inhibition of Hsp90 function and autophagy plays an important role in the suppression of tumors. DCZ5248, as a dual inhibitor of Hsp90 and autophagy, simultaneously disrupts multiple oncogenic signaling cascades, which makes it different from traditional antitumor approaches such as kinase inhibition that selectively disrupts only one or a few oncogenic signaling pathways. Chemotherapeutic regimens, including 5-FU, capecitabine, irinotecan, and oxaliplatin, are often used for metastatic colon cancer, and autophagy always accompanies radio- or chemotherapy to weaken the antitumor effect [44]. We have previously discussed that DCZ5248 could serve as a sensitizer of colon cancer to different therapies. Furthermore, in the treatment of colon cancer, chemotherapy-refractory advanced tumor progression or even acquired drug resistance occurs, such as activating B-RAF (V600E) mutations. Both inhibition of Hsp90 and autophagy can remain effective for advanced tumors [45–47]. Thus, DCZ5248 can also overcome the drug resistance of advanced colon cancer. The inhibition of tumor growth by DCZ5248 in HT-29 tumor xenografts did not meet our expectations, which may be due to poor water solubility and poor absorption in vivo. Next, we should improve the compounds' water solution and absorption in vivo through structural optimization for a lead compound. Our work provides a model to illustrate the mechanism of a novel dual Hsp90 and autophagy inhibitor exerting antitumor activity and a basis for new strategies against colon cancer.

ACKNOWLEDGEMENTS

This research was supported by grants from the National Natural Science Foundation of China (No. 81273546), the Science and Technology Commission of Shanghai Municipality (No. 18DZ2293200) and the Yunnan Province Sciences and Technology plan (No. 2017ZF010).

AUTHOR CONTRIBUTIONS

LGL and WLZ conceived the project; XLC wrote the manuscript, performed the experiments, and analyzed the data; PL synthesized the compound DCZ5248.

ADDITIONAL INFORMATION

The online version of this article (https://doi.org/10.1038/s41401-020-0398-2) contains supplementary material, which is available to authorized users.

Competing interests: The authors declare no competing interests.

REFERENCES

1. Isaacs JS, Xu WP, Neckers L. Heat shock protein 90 as a molecular target for cancer therapeutics. Cancer Cell. 2003;3:213–7.
2. Jhaveri K, Ochiana SO, Dunphy MP, Gerecitano JF, Corben AD, Peter RI, et al. Heat shock protein 90 inhibitors in the treatment of cancer: current status and future directions. Expert Opin Investig Drugs. 2014;23:611–28.

3. Li L, Wang L, You QD, Xu XL. Heat shock protein 90 inhibitors: an update on achievements, challenges, and future directions. J Med Chem 2020; 63:1798–822
4. Thorburn A, Thamm DH, Gustafson DL. Autophagy and cancer therapy. Mol Pharmacol. 2014;85:830–8.
5. Mizushima N. Autophagy: process and function. Genes Dev. 2007;21:2861–73.
6. Chen Y, Yu L. Recent progress in autophagic lysosome reformation. Traffic. 2017;18:358–61.
7. Chen F, Song Q, Yu Q. Axl inhibitor R428 induces apoptosis of cancer cells by blocking lysosomal acidification and recycling independent of Axl inhibition. Am J Cancer Res. 2018;8:1466–82.
8. Yue ZY, Jin SK, Yang CW, Levine AJ, Heintz N. Beclin 1, an autophagy gene essential for early embryonic development, is a haploinsufficient tumor suppressor. Proc Natl Acad Sci USA. 2003;100:15077–82.
9. Amaravadi RK, Lippincott-Schwartz J, Yin XM, Weiss WA, Takebe N, Timmer W, et al. Principles and current strategies for targeting autophagy for cancer treatment. Clin Cancer Res. 2011;17:654–66.
10. Liu P, Chen X, Zhu J, Li B, Chen Z, Wang G, et al. Design, synthesis and pharmacological evaluation of novel Hsp90N-terminal inhibitors without induction of heat shock response. ChemistryOpen. 2019;8:344–53.
11. Chen XL, Liu P, Wang QR, Li Y, Fu L, Fu HY, et al. DCZ3112, a novel Hsp90 inhibitor, exerts potent antitumor activity against HER2-positive breast cancer through disruption of Hsp9O-Cdc37 interaction. Cancer Lett. 2018;434: 70–80.
12. Mimnaugh EG, Chavany C, Neckers L. Polyubiquitination and proteasomal degradation of the p185(c-erbB-2) receptor protein-tyrosine kinase induced by geldanamycin. J Biol Chem. 1996;271:22796–801.
13. Zhao ZX, Zhu JM, Quan HT, Wang GM, Li B, Zhu WL, et al. X66, a novel N-terminal heat shock protein 90 inhibitor, exerts antitumor effects without induction of heat shock response. Oncotarget. 2016;7:29648–63.
14. Mathew R, Karp CM, Beaudoin B, Vuong N, Chen G, Chen HY, et al. Autophagy suppresses tumorigenesis through elimination of p62 (vol 137, 1062, 2009). Cell. 2011;145:322-.
15. Pankiv S, Clausen TH, Lamark T, Brech A, Bruun JA, Outzen H, et al. p62/SQSTM1 binds directly to Atg8/LC3 to facilitate degradation of ubiquitinated protein aggregates by autophagy. J Biol Chem. 2007;282:24131–45.
16. Patel HJ, Modi S, Chiosis G, Taldone T. Advances in the discovery and development of heat-shock protein 90 inhibitors for cancer treatment. Expert Opin Drug Dis. 2011;6:559–87.
17. Taldone T, Gozman A, Maharaj R, Chiosis G. Targeting Hsp90: small-molecule inhibitors and their clinical development. Curr Opin Pharmacol. 2008;8: 370–4.
18. Mori M, Hitora T, Nakamura O, Yamagami Y, Horie R, Nishimura H, et al. Hsp90 inhibitor induces autophagy and apoptosis in osteosarcoma cells. Int J Oncol. 2015;46:47–54.
19. He W, Ye X, Huang X, Lel W, You L, Wang L, et al. Hsp90 inhibitor, BIIB021, induces apoptosis and autophagy by regulating mTOR-Ulk1 pathway in imatinib-sensitive and -resistant chronic myeloid leukemia cells. Int J Oncol. 2016;48:1710–20.
20. Liu KS, Liu H, Qi JH, Liu QY, Liu Z, Xia M, et al. SNX-2112, an Hsp90 inhibitor, induces apoptosis and autophagy via degradation of Hsp90 client proteins in human melanoma A-375 cells. Cancer Lett. 2012;318:180–8.
21. Shen HM, Mizushima N. At the end of the autophagic road: an emerging understanding of lysosomal functions in autophagy. Trends Biochem Sci. 2014;39:61–71.
22. Menon MB, Kotlyarov A, Gaestel M. SB202190-induced cell type-specific vacuole formation and defective autophagy do not depend on p38 MAP kinase inhibition. PLoS ONE. 2011;6:e23054.
23. Amaravadi RK, Yu D, Lum JJ, Bui T, Christophorou MA, Evan GI, et al. Autophagy inhibition enhances therapy-induced apoptosis in a Myc-induced model of lymphoma. J Clin Invest. 2007;117:326–36.
24. Rao R, Balusu R, Fiskus W, Mudunuru U, Venkannagari S, Chauhan L, et al. Combination of pan-histone deacetylase inhibitor and autophagy inhibitor exerts superior efficacy against triple-negative human breast cancer cells. Mol Cancer Ther. 2012;11:973–83.
25. Dong ZW, Liang S, Hu J, Jin WY, Zhan QL, Zhao KW. Autophagy as a target for hematological malignancy therapy. Blood Rev. 2016;30:369–80.
26. Carew JS, Espitia CM, Esquivel JA, Mahalingam D, Kelly KR, Reddy G, et al. Lucanthone is a novel inhibitor of autophagy that induces cathepsin D-mediated apoptosis. J Biol Chem. 2011;286:6602–13.
27. Chikh A, Sanza P, Raimondi C, Akinduro O, Warnes G, Chiorino G, et al. iASPP is a novel autophagy inhibitor in keratinocytes. J Cell Sci. 2014;127:3079–93.
28. Kim DG, Jung KH, Lee DG, Yoon JH, Choi KS, Kwon SW, et al. 20(*S*)-Ginsenoside Rg (3) is a novel inhibitor of autophagy and sensitizes hepatocellular carcinoma to doxorubicin. Oncotarget. 2014;5:4438–51.
29. Shao S, Li S, Qin YW, Wang XR, Yang YN, Bai HT, et al. Spautin-1, a novel autophagy inhibitor, enhances imatinib-induced apoptosis in chronic myeloid leukemia. Int J Oncol. 2014;44:1661–8.
30. Sheng Y, Sun B, Guo WT, Liu X, Wang YC, Xie X, et al. (4-[6-(4-Isopropoxyphenyl) pyrazolo[1,5-a]pyrimidin-3-yl] quinoline) is a novel inhibitor of autophagy. Br J Pharmacol. 2014;171:4970–80.
31. Wang ZH, Zhang J, Wang Y, Xing R, Yi CQ, Zhu HS, et al. Matrine, a novel autophagy inhibitor, blocks trafficking and the proteolytic activation of lysosomal proteases. Carcinogenesis. 2013;34:128–38.
32. Zhao XJ, Fang Y, Yang Y, Qin Y, Wu P, Wang T, et al. Elaiophylin, a novel autophagy inhibitor, exerts antitumor activity as a single agent in ovarian cancer cells. Autophagy. 2015;11:1849–63.
33. He S, Smith DL, Sequeira M, Sang J, Bates RC, Proia DA. The HSP90 inhibitor ganetespib has chemosensitizer and radiosensitizer activity in colorectal cancer. Invest New Drugs 2014;32:577–86.
34. Fennell D, Danson S, Forster M, Talbot D, Woll P, Child J, et al. Phase 1 study of HSP90 inhibitor ganetespib with pemetrexed and cisplatin/carboplatin chemotherapy for pleural mesothelioma. J Thorac Oncol. 2018;13:S397-S.
35. Johnson ML, Yu HA, Hart EM, Weitner BB, Rademaker AW, Patel JD, et al. Phase I/II study of HSP90 inhibitor AUY922 and Erlotinib for EGFR-mutant lung cancer with acquired resistance to epidermal growth factor receptor tyrosine kinase inhibitors. J Clin Oncol. 2015;33:1666–73.
36. Nti AA, Serrano LW, Sandhu HS, Uyhazi KE, Edelstein ID, Zhou EJ, et al. Frequent subclinical macular changes in combined Braf/Mek inhibition with high-dose hydroxychloroquine as treatment for advanced metastatic Braf mutant melanoma: preliminary results from a phase I/II clinical treatment trial. Retina. 2019;39:502–13.
37. Rangwala R, Chang YC, Hu J, Algazy KM, Evans TL, Fecher LA, et al. Combined MTOR and autophagy inhibition: phase I trial of hydroxychloroquine and temsirolimus in patients with advanced solid tumors and melanoma. Autophagy. 2014;10:1391–402.
38. Rangwala R, Leone R, Chang YC, Fecher LA, Schuchter LM, Kramer A, et al. Phase I trial of hydroxychloroquine with dose-intense temozolomide in patients with advanced solid tumors and melanoma. Autophagy. 2014;10:1369–79.
39. Rosenfeld MR, Ye X, Supko JG, Desideri S, Grossman SA, Brem S, et al. A phase I/II trial of hydroxychloroquine in conjunction with radiation therapy and concurrent and adjuvant temozolomide in patients with newly diagnosed glioblastoma multiforme. Autophagy. 2014;10:1359–68.
40. Smith DL, Acquaviva J, Sequeira M, Jimenez JP, Zhang CH, Sang J, et al. The HSP90 inhibitor ganetespib potentiates the antitumor activity of EGFR tyrosine kinase inhibition in mutant and wild-type non-small cell lung cancer. Target Oncol. 2015;10:235–45.
41. Kong A, Rea D, Ahmed S, Beck JT, Lopez RL, Biganzoli L, et al. Phase 1B/2 study of the HSP90 inhibitor AUY922 plus trastuzumab in metastatic HER2-positive breast cancer patients who have progressed on trastuzumab-based regimen. Oncotarget. 2016;7:37680–92.
42. Smyth T, Paraiso KHT, Hearn K, Rodriguez-Lopez AM, Munck JM, Haarberg HE, et al. Inhibition of HSP90 by AT13387 delays the emergence of resistance to BRAF inhibitors and overcomes resistance to dual BRAF and MEK inhibition in melanoma models. Mol Cancer Ther. 2014;13:2793–804.
43. Mielczarek-Lewandowska A, Sztiller-Sikorska M, Osrodek M, Czyz M, Hartman ML. 17-Aminogeldanamycin selectively diminishes IRE1-XBP1s pathway activity and cooperatively induces apoptosis with MEK1/2 and BRAF(V600E) inhibitors in melanoma cells of different genetic subtypes. Apoptosis. 2019;24:596–611.
44. El Zouhairi M, Charabaty A, Pishvaian MJ. Molecularly targeted therapy for metastatic colon cancer: proven treatments and promising new agents. Gastrointest Cancer Res. 2011;4:15–21.
45. Vasilevskaya IA, O'Dwyer PJ. 17-allylamino-17-demethoxygeldanamycin overcomes TRAIL resistance in colon cancer cell lines. Biochem Pharmacol. 2005; 70:580–9.
46. Goulielmaki M, Koustas E, Moysidou E, Vlassi M, Sasazuki T, Shirasawa S, et al. BRAF associated autophagy exploitation: BRAF and autophagy inhibitors synergise to efficiently overcome resistance of BRAF mutant colorectal cancer cells. Oncotarget. 2016;7:9188–221.
47. Wang CY, Guo ST, Wang JY, Liu F, Zhang YY, Yari H, et al. Inhibition of HSP90 by AUY922 Preferentially Kills Mutant KRAS Colon Cancer Cells by Activating Bim through ER Stress. Mol Cancer Ther. 2016;15:448–59.